Title

Arginine culture turns on the elusive nitrogen starvation signal during robust phototrophic growth in *Chlamydomonas*

Authors

Jacob Munz[1], Yuan Xiong[1], Thamali Kariyawasam[1], Nolan Shelley[1], Jenny Lee[1], Ran Ha Hong[1], Jaoon Young Hwan Kim[2], Young Joon Sung[3], Seung-Bum Seo[4], Sang Jun Sim[3], EonSeon Jin[4], and Jae-Hyeok Lee[1]

Address

1. Department of Botany, University of British Columbia, Vancouver, British Columbia V6T1Z4, Canada
2. Convergence Research Division, National Marine Biodiversity Institute of Korea, Chungcheongnam-do 33662, Republic of Korea.
3. Department of Chemical and Biological Engineering, Korea University, Seoul 136-713, Republic of Korea
4. Department of Life Sciences, Research Institute for Natural Sciences, Hanyang University, Seoul 133-791, Republic of Korea

E-mail address

Jacob Munz: jack.munz@botany.ubc.ca
Yuan Xiong: yuan.xiong@botany.ubc.ca
Thamali Kariyawasam: thamali.kariyawasam@botany.ubc.ca
Nolan Shelley: nolan.shelley@botany.ubc.ca
Jenny Lee: jnylee208@hotmail.com
Ran Ha Hong: lhonglana372@hotmail.com
Jaoon Young Hwan Kim: jaoonkim@gmail.com
Young Joon Sung: solrorica@naver.com
Seung-Bum Seo: sbseo001@daum.net
Sang Jun Sim: simsj@korea.ac.kr
EonSeon Jin: esjin@hanyang.ac.kr

Corresponding Author:
Jae-Hyeok Lee
#1326C-6270 University Blvd.
1-604-827-5973
jae-hyeok.lee@botany.ubc.ca

Date of submission: September 13th, 2018
The number of figures: 8
The number of tables: 2
Word count: 6409 words
Supplementary data: 6 figures and 3 tables

Title

Arginine culture turns on the elusive nitrogen starvation signal during robust phototrophic growth in *Chlamydomonas*

Running title

Arginine decouples N starvation responses from growth arrest

Highlights

Arginine catabolism leads to the activation of nitrogen starvation responses while supporting robust photosynthesis and growth, presenting ways to investigate N starvation signaling mechanisms in photosynthetic organisms.

Abstract

Under nitrogen (N) starvation, photosynthetic organisms search for other N sources while slowing down photosynthesis by downregulating light harvesting and electron transport to balance the carbon/nitrogen ratio and eventually stopping growth due to N limitation. To investigate the elusive N starvation-specific signaling mechanisms, we sought a way to induce N starvation responses without limiting photosynthesis or cell growth. In the chlorophyte *Chlamydomonas reinhardtii*, gametogenesis is exclusively induced during N starvation except in arginine culture. We showed that the arginine-grown culture turned on N starvation responses including hundreds-fold induction of N starvation-induced genes, reduced chlorophyll content, and increased carbon storage in the form of lipid droplets. Arginine culture supported robust phototrophic growth but not heterotrophic growth, indicating that arginine catabolism contributes CO_2 to Rubisco without directly fueling ATP synthesis. Based on *in silico* analysis, we propose the possible routes of arginine catabolism that may bypass critical steps for monitoring of cellular N status and thereby trigger N starvation responses. Our results describe a study system where the N starvation responses are constantly induced without compromising

photosynthesis or growth, paving ways to discover the mechanisms that sense and respond to cellular N status in eukaryotic phototrophs.

Keywords:
Arginine catabolism, Chlamydomonas, Nitrogen catabolite repression, Nitrogen starvation, Phototrophic growth, Nitrogen signaling

Abbreviations:
ADC = arginine decarboxylase
ADI = arginine deiminase
CCM = carbon concentrating mechanism
DCMU = 3-(3,4-dichlorophenyl)-1,1-dimethylure
FA = fatty acid
FAME = fatty acid methyl ester
NCR = nitrogen catabolite repression
TAG = triacylglycerol
TAP = tris-acetate-phosphate medium

Introduction

All living organisms require constant nitrogen (N) supply for their growth and survival. Two adaptive strategies are generally considered when N sources are not in sufficient supply: 1) to search for new N sources by inducing high-affinity transporters and/or by changing growth patterns or chemotaxis, known collectively as N scavenging, and 2) to mobilize internal N reserves such as storage proteins and N-rich molecules, known collectively as N salvaging (Ono *et al.,* 1996; Chalker-Scott, 1999; Ding *et al.,* 2005; Diaz *et al.,* 2006). Expression of genes involved in N scavenging and N salvaging are suppressed when preferred N sources are available. This regulation has been described as nitrogen catabolite repression (NCR) and its molecular mechanisms have been studied in detail using *Saccharomyces cerevisiae* as a model (Cooper, 1982; reviewed in Zhang *et al.,* 2018).

N homeostasis of photosynthetic organisms is challenging as they acquire N primarily from inorganic N sources such as nitrate (NO_3^-) and ammonium (NH_4^+). Assimilation of inorganic N sources requires a significant amount of carbon skeletons and reducing equivalents thereby becoming a primary sink of photosynthetic products. Photosynthetic organisms must coordinate N assimilation and photosynthesis which has been documented in microalgae. Abrupt N deprivation predicts the accumulation of high-energy electrons that are otherwise used for N assimilation (reviewed in Turpin *et al.,* 1988). Such a redox imbalance can be reversed by diverting excess high-energy electrons to a new sink such as carbon storage molecules including starch and triacylglycerol (TAG) as a protective response (Li *et al.*, 2012; Johnson & Alric, 2013). Conversely, N assimilation is inhibited when high-energy electron donors are in low abundances, such as during the dark phase or when limited exogenous carbon sources are provided in the absence of photosynthesis (Syrett, 1953a; Syrett, 1953b; Amory *et al.,* 1991; Huppe & Turpin, 1994).

Triggering N limitation responses requires signaling mechanisms that sense external and internal N availabilities. Using *Chlamydomonas reinhardtii* as a system, transcriptional/proteomic changes upon N starvation have been intensely studied in the interest of knowing the trigger and routes of TAG accumulation in microalgae (Lee *et al.,* 2012, Wase *et al.,* 2014). N limitation rapidly induces genes including the common N catabolite genes for N scavenging and N salvaging, suggesting that *C. reinhardtii* actively remobilizes N from purines and amino acids while searching for alternative external N sources (Schmollinger *et al.,* 2014; Park *et al.,* 2015). N limitation also downregulates photosynthesis genes including the majority of antenna and photosystem genes (39 out of 42 in Miller *et al.,* 2010). It remains to be studied whether transcriptional or post-transcriptional level regulations are involved in the rapid changes in gene expression upon N limitation.

Physiological responses to N limitation in *C. reinhardtii* include the transition to sexually competent gametes (gametogenesis), degradation of photosynthetic proteins/chlorophylls, ribosome turnover, and the accumulation of carbon storage molecules (Sager & Granick, 1954; Siersma & Chiang, 1971; Martin & Goodenough, 1975; Bulté & Wollman, 1992; Weers & Gulati, 1997). Of which, gametogenesis is a response unique to N starvation as the removal of any single component other than N from the growth medium does not elicit this response. Cultures produce <1% sexually competent gametes when the preferred N sources, NH_4^+ or NO_3^-, are present (Sager & Granick, 1954; Matsuda *et al.,* 1992; Pozuelo *et al.,* 2000).

C. reinhardtii can grow on various N sources ranging from simple NH_4^+ and amino acids to complex nucleic acids and their derivatives (Sager & Granick, 1953; Cain, 1965). Muñoz-Blanco *et al.,* (1990) reported that twelve amino acids can serve as the sole N source for *C. reinhardtii* growth. The primary route of entry for these amino acids is extracellular deamination via L-amino acid oxidase, encoded by *LAO1*, releasing NH_4^+ (Muñoz-Blanco *et al.,* 1990; Piedras *et al.,*

1992; Vallon *et al.,* 1993). As an exception, arginine is reported to enter the cells by a specific active transporter system (Kirk & Kirk, 1978) whose molecular identity and exact substrate specificity is unknown. Interestingly, arginine is the only N source reported to produce gametes while retaining a culture growth rate comparable to the preferred N sources (Honeycutt & Margulies, 1972). It was later demonstrated that arginine-grown cells remain gametic following mitosis and continue cell cycle progression (Matsuda *et al.,* 1992). These studies suggest that the occurrence of gametes in arginine grown populations is not due to lacking N but rather to the lack of a repressive gametogenesis signal such as NH_4^+. How arginine culture induces gametogenesis was not thoroughly investigated.

We present in this study the physiological and molecular responses of *C. reinhardtii* cultures grown in arginine-based media. We report that arginine cultures activate a suite of N catabolite genes together with N starvation-induced responses such as gametogenesis, chlorophyll degradation, and TAG accumulation while supporting comparable growth to NH_4^+. Similar induction of TAG accumulation in arginine cultures of a diatom, *Phaeodactylum tricornutum*, suggests that arginine feeding alleviates canonical NCR and provides a fruitful approach to investigate N starvation responses without growth arrest in microalgae.

Materials and methods

Strains and culture conditions

Chlamydomonas reinhardtii wild-type strains, 137c (cc125: *nit1; nit2; mt*+) and 21gr (cc1690: *NIT1; NIT2; mt*+), and the *cia5* mutant (cc4427) were obtained from the Chlamydomonas Center (https://www.chlamycollection.org/). All strains were mixotrophically grown in Tris-acetate-phosphate (TAP) medium (Gorman & Levine, 1965) containing 8 mM ammonium chloride (NH_4Cl), 8 mM L-arginine, or

no nitrogen. Acetate was omitted for all autotrophic and heterotrophic growth experiments. All strains were cultured under low light (30 µmol m^{-2} s^{-1}) at 23°C unless otherwise stated. Growth curves were established using a small scale photobioreactor (Multi-Cultivator MC1000; Photon System Instruments, Czech Republic) measuring the absorption at 680 nm every five minutes with an initial cell concentration of 2 x 10^5 cells mL^{-1}.

Axenic stocks of *Phaeodactylum tricornutum* Bohlin (CCMP632) were obtained from the National Center for Marine Algae and Microbiota at the Bigelow Laboratory for Ocean Sciences. Diatom cells were cultured in f/2+Si medium (enriched artificial seawater) containing 10 mM sodium bicarbonate. Sodium nitrate ($NaNO_3$) in the standard f/2+Si medium was replaced by the amount of arginine calculated from the molar concentration of nitrogen in standard medium. Cultures were grown on an orbital shaker at 20°C under a 12 h/12 h light/dark regime.

Measurement of gametogenesis

Cells were cultured for ten days with either NH_4^+ or arginine as the N source. Cells were then resuspended in 1 mL of fresh NH_4^+ or arginine TAP liquid culture to a final density of 2 x 10^6 cells mL^{-1} and incubated in a 24-well plate for 24 hours. Cells (2 x 10^7) from the NH_4^+-TAP plate for each strain and for the high mating efficiency minus strain, cc621, were resuspended in N-free TAP six hours prior to measurements to induce gametogenesis and serve as controls and mating partner, respectively (N-free controls in Fig. S1). Mating efficiency was measured by mixing an equal number of experimental cells with the cc621 tester gametes and counting the percent of fused quadri-flagellated cells out of 200 cells after a 30-minute incubation in low light (30 µmol m^{-2} s^{-1}), as in Galloway & Goodenough, 1985.

Selection of N limitation marker genes

We collected N starvation marker genes representing N scavenging (ex. *DUR3A*, *NRT2.1*, and *LAO1*) and N salvage (ex. *AIH2*, *AMT4*, and *GLN3*), which were previously shown to be upregulated between 100 and 1000-fold within two hours of N starvation with stably low basal expression (Schmollinger *et al.,* 2014; Table S1). Three expression patterns distinguish N starvation marker genes: 1) Continue expression once induced early in N starvation, 2) Transient expression going back to basal expression within two hours of N starvation, and 3) Also induced by NO_3^- in a NIT2-dependent manner. We selected two or three genes from each category that displayed the most robust upregulation under N starvation in the available transcriptome sets (Table S1).

Reverse transcription quantitative PCR (RT-qPCR)

Liquid precultures (100 mL) of NH_4^+ or arginine TAP were inoculated to a concentration of 2 x 10^5 cells mL^{-1} and grown to mid-log phase (2 - 8 x 10^6 cells mL^{-1}). Fresh cultures (100 mL) of the same media type were inoculated again to a concentration of 2 x 10^5 cells mL^{-1} using the mid-log phase precultured cells acclimated to either NH_4^+ or arginine. At mid-log phase the cultures were harvested at 3,000 rpm for 3 minutes and washed twice with 50 mL N-free TAP. Washed cells were added to 25 mL of arginine, NH_4^+, or N-free TAP in a petri dish to a final concentration of 2 x 10^6 cells mL^{-1} and incubated for 2 hours or 24 hours. RNA extraction and RT-qPCR were performed as previously described (Joo et al., 2017). All qPCR experiments were normalized to the endogenous reference gene *CBLP* which has been commonly used for normalization in *C. reinhardtii,* including long-term N starvation (Allen *et al*., 2007; Tsai *et al*., 2014). Samples were run in duplicate for three biological replicates and one tech replicate was run on a gel to confirm one single band of the correct length. Primer sequences and amplicon lengths are presented in Table S1.

Chlorophyll fluorescence and photosynthetic parameter measurements

Cells were grown in 50 mL cultures in a 250 mL beaker covered with a petri dish under low light (30 µmol m^{-2} s^{-1}) or high light (150 µmol m^{-2} s^{-1}) for mixotrophic and phototrophic studies, respectively. Log phase cultures were sampled, 2 - 8 x 10^6 cells mL^{-1} for mixotrophic cultures and 2 - 5 x 10^6 cells mL^{-1} for phototrophic cultures. *In vivo* chlorophyll fluorescence was measured with a JTS-10 spectrophotometer (Bio-Logic Science Instruments, France) and recorded with a CCD camera (C9300-221, Hamamatsu, Japan) (Johnson *et al.,* 2009). Samples were incubated in dark for 10 minutes prior to fluorescence measurements. Maximum quantum efficiency of PSII photochemistry (F_v / F_m) and PSII operating efficiency (F_q' / F_m'; Φ_{PSII}) were calculated as F_m - F_o / F_o and F_m' - F / F_m', respectively (reviewed in Baker, 2008). PSII functional antenna size was estimated as described before (Bianchi *et al.,* 2008). Samples were incubated in dark for 5 min followed by incubating with 10 µM of 3-(3,4-dichlorophenyl)-1,1-dimethylurea (DCMU) for 10 min in dark. Fluorescence induction curves were induced by green actinic light of 23 µmol m^{-2} s^{-1}. The time for variable fluorescence (F_s) to reach 2/3 of maximum fluorescence (F_m) is inversely proportional to the PSII functional antenna size. Chlorophyll was extracted in 80% acetone and cell debris removed by centrifuging at 20,000x*g* for 5 minutes (Kirst *et al.,* 2012). Chlorophyll was quantified according to Arnon, 1949 by examination of supernatant light absorbance at 645 nm, 665 nm and 720 nm with a spectrophotometer (DU 730, Beckman Coulter, USA) and correcting equations as in Melis *et al.,* (1987). Oxygen evolution rate was measured using a Clark-type electrode (Hansatech Oxygraph Plus, Hansatech Instruments Ltd, England) with intact cells diluted to a concentration of 10 µg total chlorophyll mL^{-1}. Samples were treated with 10 mM of HCO_3^- for 10 minutes before oxygen evolution measurement. Oxygen evolution rate was measured under following actinic light: 100, 200, 400, and 700 µmol m^{-2} s^{-1}.

Microscopy

Images of *Chlamydomonas* cells were captured with a Leica DFC350 FX camera mounted on a Leica DM6000 B microscope with a 100x oil immersion lens objective. Starch granules were visualized using differential interference contrast. Lipid droplets were stained with Nile red (Sigma-Aldrich, USA) at a final concentration of 1 µg mL^{-1} with a 20 min dark, room temperature incubation . A 488 nm excitation and a 560 to 600 nm emission wavelength were used to capture the Nile red signal. *P. tricornutum* lipid droplets were stained by adding Nile red stock (0.1 mg mL^{-1} in acetone) into cell culture (1:50) and a 10 min dark, room temperature incubation. 1% low melting agarose was mixed with the treated cultures (1:1). Stained cells were observed under a laser-scanning confocal microscope, ECLIPSE Ti (Nikon Corp.) using 561 nm excitation wavelength and a long-pass 570 nm emission filter. The images were captured from representative cells.

Analysis of neutral lipid content

To quantify the TAG of *C. reinhardtii* cultures (21gr and *sta*6), cell suspension was concentrated to 1 x 10^8 cells mL^{-1}. Cellular and subcellular fractions were extracted with methanol-chloroform-formic acid mixture (2:1:0.1, v/v) and phases were separated by adding 0.5 ml of 1 M potassium chloride (KCl) and 0.2 M phosphate (H_3PO_4) solution. The organic phase was loaded on silica gel matrix aluminum plates (20 x 20 cm, Sigma-Aldrich, USA) immersed in 0.15 M ammonium sulfate solution for 30 minutes and dried for at least 2 days. Lipids were separated on a thin layer chromatography (TLC) plate using a double development solvent system (2/3 in acetone-toluene-water (91:30:3, v/v)) and then fully in hexane-diethyl ether-acetic acid (70:30:1, v/v) in a sealed container. TAGs were identified using a soybean lipid profile as a reference and scraped off the TLC plate. The scraped lipids and silica were transferred to a screw cap glass tube and 1 mL of hexane was added. For the total fatty acid methyl ester (FAME) analysis, total lipids were extracted by the Bligh-Dyer method (Bligh & Dyer, 1959) as described in more detail (Kim *et al.,* 2016). For gas

chromatography analysis, pentadecanoic acid (C15:0) was added to 1 mg mL^{-1} as an internal standard. All samples were methylated by acid-catalyzed transesterification using methanol with sulfuric acid (3%, v/v) and heated at 95°C for 1.5 hours (Lim *et al.,* 2014). After collection of the organic phase, FAMEs were analyzed using gas chromatography (Agilent 7890A) with a flame ionization detector and a DB-23 column (Agilent, USA) with the following working conditions: injection volume, 1 µL; split ratio, 1:50; inlet temp, 250°C; detector temp, 280°C; oven temp, hold at 50°C for 1 min, increase to 175°C at 25°C min^{-1}, increase to 230°C at 4°C min^{-1}, and hold for 5 min. The amounts of TAG and FAME were quantified based on the number of cells extracted.

For *P. tricornutum* experiments, cells were cultured for 10 days and then incubated in N-free f/2+Si medium for 3 days. The cultures were then inoculated in f/2+Si medium with $NaNO_3$ or arginine medium as the N source. *P. tricornutum* lipid relative quantification with Nile red was performed as in Xue *et al.,* 2015. Cells were treated with 20% DMSO for 20 min followed by the addition of 10 µL Nile red stock (0.1 mg mL^{-1} in acetone) to 1 mL of pretreated culture, inverting rapidly. Samples were incubated in the dark for 20 min at room temperature. 200 µL of stained culture was transferred to a black well plate. The fluorescence was detected in Varioskan Flash spectral scanning multimode reader (Thermo Fisher Scientific, USA) with the excitation wavelength of 530 nm and the emission wavelength of 580 nm. Relative fluorescence was divided by cell concentration which was determined by hemocytometer.

Results

N starvation-induced genes are upregulated in arginine cultures that display gametogenesis during robust growth

Previous reports demonstrating the role of arginine in inducing gametogenesis primarily relied on one genetic background, 137c (Honeycutt & Margulies, 1972;

Matsuda *et al.,* 1992), which is incapable of growth using NO_3^- as the sole N source. We first questioned whether gametogenesis induced in arginine cultures requires specific genetic backgrounds by comparing the field isolated strains 21gr (cc1690: *NIT1; NIT2*) and 137c (cc125: *nit1; nit2*) that differ in the nitrate reductase (*NIT1*) and the RWP-RK transcription factor regulating nitrate assimilation genes (*NIT2*). Both strains maintained ~10% of gamete populations in pre-acclimated arginine cultures in contrast to little or no gametes in NH_4^+-based cultures (Fig. 1A). We also examined four natural isolates of *C. reinhardtii* (Fig. S2) that confirmed gametogenesis is a general response to arginine culturing and is not dependent on specific genetic backgrounds. Next, we examined if the arginine cultures experience any limitation in growth. Arginine was found to be an efficient N source supporting comparable cell proliferation and final density when growth rate was monitored in a bioreactor alongside NH_4^+ cultures (Fig. 1B & 1C).

With this premise, we further investigated whether arginine cultures activate another response unique to N starvation cultures. The earliest response to N starvation is the rapid upregulation of N starvation-inducible genes within 0.5 - 2 hours after removal of preferred N sources (Schmollinger *et al.,* 2014). We selected eight N starvation marker genes representing N scavenging and N salvaging (Table S1). All eight marker genes were highly upregulated, comparable to N-deprived cells, when NH_4^+-grown cells were transferred to arginine medium (NH_4^+ pre-, Fig. 2). Expression of five marker genes remained high after 24-hrs in arginine media, whereas expression of *AIH2*, *DUR3a,* and *LAO1* was reduced (Fig. 2; Table S1) which corresponds to their transient upregulation reported during N deprivation (Schmollinger *et al.,* 2014). *FDX2* expression reduced to the basal level in the 24-hr arginine culture of 137c strain, but not of the 21gr strain.

Next, we asked whether the observed expression of N starvation-induced genes was due to a transient cellular condition prior to acclimation in arginine medium by examining cells acclimated to arginine medium for a week. The arginine-

acclimated cells showed comparable upregulation of *AMT4, GLN3, NIT1,* and *NRT2.1* and reduced but significantly upregulated *AIH2*, *FDX2*, and *LAO1* expression. *DUR3a* was the only marker gene that displayed variable expression patterns: basal level in the 21gr strain, whereas it was upregulated in 137c strain and returned to the basal level after the transfer to N-free medium. The transfer of arginine-grown cells to N-free medium did not further upregulate these genes except for *FDX2* which showed an additional two- to three-fold induction. Nitrate assimilation genes, such as *NIT1* and *NRT2.1*, are primarily activated by NO_3^- via the NIT2 transcription factor. Their upregulation in N-free and arginine conditions was comparable between the *NIT2* wild-type strain 21gr and the *nit2*-null strain 137c (Fig. 2). We further examined NIT2-dependent transcriptional regulation using *THB1* as a marker (Johnson *et al.,* 2014) and found no upregulation of *THB1* in either N-free or arginine culture which suggests no direct involvement of NIT2-mediated regulation in the N-starvation responses invoked in the arginine cultures (Fig. S3). Together, these results suggest that the same gene regulatory mechanism triggered by N starvation becomes activated during arginine growth independently of NIT2-dependent transcriptional regulation.

Arginine grown cells have less chlorophyll but increased photosynthetic productivity

Downregulation of photosynthesis is one of the early signs of N limitation in *C. reinhardtii*. Mixotrophic arginine cultures showed a dramatic reduction in the cellular chlorophyll contents down to 66% of the levels found in NH_4^+ cultures and visibly manifested as pale green cultures (Table 1; Fig. 3A). In contrast, other photosynthesis measures such as maximum photosynthetic productivity (F_V / F_M), photosynthetic efficiency (ΦPSII), and chlorophyll a/b ratio in arginine cultures were not significantly different from those in NH_4^+ cultures. These results suggest that chlorophyll reduction is a direct response to N starvation signaling and not due to imposed stress (Table 1).

We analyzed light-dependent oxygen evolution of arginine cultures to quantify the overall photosynthesis of arginine cultures. Arginine cultures showed increased photosynthetic yield per chlorophyll compared to NH_4^+ cultures with light intensity saturation above 700 μmol m^{-2} s^{-1} (Fig. 3B & 3C). Reduced chlorophyll contents might directly affect light intensity saturation of photosynthesis by changing antenna size. We analyzed fluorescence rise kinetics in the presence of DCMU as a proxy to measure the functional antenna size of the arginine cultures. Arginine-grown cells displayed almost twice larger antenna size compared to NH_4^+-grown cells ruling out a smaller antenna size as the cause for increased photosynthetic productivity (Fig. 3D). Overall, the arginine culture showed reduced chlorophyll content without compromising the photosynthetic capacity nor reducing the antenna size.

Arginine-grown cells increase the flux of organic carbons towards storage

Lipid accumulation in response to N starvation is well documented (Hu *et al.,* 2008; Rodolfi *et al.,* 2009), however, it is not known whether N starvation triggers lipid body biogenesis directly or indirectly because of cell cycle arrest or generic stress responses. Examination of neutral lipids in logarithmic arginine cultures revealed pronounced lipid droplets in mixotrophic cultures of 137c and in both the mixotrophic and phototrophic cultures of 21gr (Fig. 4A). The relative size and number of lipid droplets found in the arginine cultures were less than those observed in cells starved of nitrogen for three days in either mixotrophic or phototrophic conditions. Strain specific differences in oil body formation could be due to variable carbon flux towards starch biosynthesis that increases during N starvation. To assess the overall carbon flux into storage molecules, we examined the *starchless* mutant, *sta6*, that diverts all storage carbons to lipids. The large number and size of lipid droplets in arginine-grown *sta6* cells attests to increased flux toward carbon storage molecules (Fig. 4A). Consistent with the Nile red staining results, the TAG contents based on gas chromatography were 27% and 317% higher in the arginine-grown cells than the NH_4^+-grown cells for

21gr and *sta6*, respectively (Fig. 4B). Quantitative analysis of the FAME content showed that TAGs account for ~20% of the cellular fatty acid (FA) content in arginine-grown *sta6* cells in contrast to <10% in NH_4^+-grown cells (Fig. 4C).

TAGs can be synthesized from *de novo* FAs or the degradation of existing lipids into FA precursors. To investigate the sources of FAs for lipid body biogenesis in arginine-grown cells, we analyzed lipid profiles of the TAGs from *sta6*. The *sta6* cultures showed increases in the proportion of *de novo* synthesized FAs, particularly 16:0 (Fig. 4D). This contrasts with the enrichment of unsaturated FAs in the lipid profiles of N starvation induced TAGs indicative of chloroplastic membrane origin (Li *et al.,* 2012). Our results suggest that N starvation signaling triggers TAG biosynthesis and shuttles available FAs into oil bodies.

Arginine catabolism relieves CO_2-limitation during phototrophic growth

Our results showed that arginine-grown cells displayed N starvation phenotypes when both gene expression and physiology were examined. An important follow up question was how arginine culture induces N starvation responses without actual N limitation. We focused on the arginine catabolic routes that may bypass intracellular N availability sensation and thereby trigger N starvation responses. Alternatively, the extra carbons available in each molecule of arginine may disrupt the C (carbon):N balance within the cell and trigger N starvation responses.

To assess whether arginine catabolism directly contributes to the organic carbon pool, we examined arginine-cultures in the absence of photosynthesis. We first determined a minimal light condition (<10 μmol m^{-2} s^{-1}) unable to support the phototrophic growth of NH_4^+ cultures with sufficient CO_2 supply (5%) (Fig. 5A). Arginine cultures did not grow under the same condition, indicating that arginine catabolism does not contribute organic carbon towards heterotrophic growth.

The inability to catabolize arginine as an organic carbon source suggests that arginine catabolism may instead produce CO_2 or feed carbon skeletons only to photosynthesis. We compared the phototrophic growth under high light (250 µmol m^{-2} s^{-1}) where CO_2 supply constrains growth to assess whether arginine cultures experience C limitation. The growth rate of both arginine and NH_4^+ cultures was significantly improved by 5% CO_2 supply (Fig. 5B & C). This suggested that arginine catabolism may not contribute sufficient CO_2 to Rubisco.

Efficient phototrophic growth under CO_2-limiting conditions relies on functional carbon concentrating mechanisms (CCM). If arginine catabolism contributes significant CO_2 to Rubisco, arginine cultures can bypass the need of CCM. To test this hypothesis, we characterized *cia5* mutant that cannot turn on the CCM under ambient CO_2 condition (Van *et al.,* 2001; Wang *et al.,* 2005). The *cia5* mutant displayed robust phototrophic growth in arginine but not NH_4^+ medium under high light (~150 µmol m^{-2} s^{-1}) (Fig. 6A). The robust *cia5* growth could be explained by an active CCM via a CIA5-independent pathway and/or an unknown mechanism that suppresses photorespiration. To assess whether the CCM becomes active in arginine cultures, we examined starch sheath formation surrounding the pyrenoid at the center of the chloroplast as the hallmark of active CCM (Ramazanov *et al.,* 1994; Moroney & Ynalvez, 2007). The majority of NH_4^+-grown cells developed a robust starch sheath in ambient CO_2, whereas the arginine-grown cells formed an incomplete or no starch sheath indicating that the CCM is not fully operating in arginine cultures (Fig. 6B). These results suggest that arginine cultures may produce a significant CO_2 concentration enough for efficient Rubisco activity independently from the CIA5-dependent CCM.

N starvation marker genes are upregulated in phototrophic arginine cultures

We examined phototrophic arginine cultures for N starvation responses as it appears evident that arginine culture affects carbon fixation. The phototrophic arginine cultures upregulated N starvation marker genes by 100-100,000-fold like

the mixotrophic cultures (Fig. S4). One exception is *LAO1* which was not upregulated in the arginine-grown 21gr strain. All measures related to photosynthesis including cellular chlorophyll contents were found comparable between the NH_4^+ and arginine cultures in phototrophic conditions (Table 2). The only noticeable difference was a two-fold increase in the oxygen evolution rate in the arginine cultures, which was also observed in mixotrophic cultures (Fig. S5). Improved C-fixation efficiency may explain increased photosynthetic productivity with marginal improvements of F_V / F_M and PSII operating efficiency in the arginine cultures.

Genome survey suggests that arginine catabolism is confined in the chloroplast

Our results so far suggested that arginine catabolism bypasses the N-status monitoring system and does not directly contribute to the cellular C content but promotes photosynthetic efficiency by an unknown mechanism. Therefore, we investigated plausible routes of arginine catabolism according to those present in the *C. reinhardtii* genome. Higher plants use arginine as a N storage molecule whose utilization is primarily dependent on arginase activity that is lacking in *C. reinhardtii* (reviewed in Winter *et al.,* 2015). Similarly, no gene or protein activity has been found in *C. reinhardtii* for arginine-dependent nitric oxide synthase. This leaves two possible enzymatic pathways for arginine catabolism: one begins with arginine deiminase (ADI) and the second with arginine decarboxylase (ADC). All candidate genes involved in arginine catabolism are listed in Table S2.

Activity of the ADI pathway was observed when cells were grown in arginine and was therefore reported as the major route (Sussenbach & Strijkert, 1969). ADI is predicted to be localized to the chloroplast together with the arginine biosynthesis pathway (Table S2). ADI cleaves the amine group from the ureido group of arginine to produce citrulline and NH_4^+ (Oginsky & Gehrig, 1952; Petrack *et al.,* 1957). Citrulline may be further processed into ornithine and carbamoyl phosphate by the single ornithine carbamoyltransferase (OTC) in *C. reinhardtii*.

However, the *otc1*-null mutant, *arg4,* was shown to grow well with arginine as the sole N source, indicating a minor role of OTC in arginine catabolism (Loppes, 1969). A later study reported that the majority of citrulline was degraded into organic acids without releasing ornithine, NH_4^+, or CO_2 which thereby excluded OTC and citrulline hydrolase from the candidate pathway of arginine catabolism (Sussenbach & Strijkert, 1970).

The evidence supporting the ADC pathway is much weaker. ADC cleaves the carboxyl group of the amino acid group releasing agmatine and CO_2. ADC homologs have been reported in plants and several *Chlorella* species but not in *C. reinhardtii* (Cohen *et al.,* 1983; Bell & Malmberg, 1990; Hanfrey *et al.,* 2001). If present, we consider the ADC pathway to play a minor role from the following observations. First, the agmatine catabolic enzymes, encoded by two agmatine hydrolase genes (*AIH1* and *AIH2*), are predicted to localize to the mitochondria meaning the ADC pathway would likely be directed to the mitochondria (Table S2). However, our evidence of increased photosynthetic productivity and mitigation of requisite CCM in ambient CO_2 during arginine culture argue towards chloroplastic catabolism for arginine (Fig. 3B, C & 6). Secondly, the upregulation of *AIH2* in N-starved and arginine conditions was transient (Fig. 2) (Schmollinger *et al.,* 2014). We propose that the ADI-Citrulline degradation pathway is the most likely metabolic route of providing necessary N molecules during arginine-dependent growth (pathway A in Fig. 7).

Arginine-induced lipid accumulation occurs in the diatom Phaeodactylum

Nitric oxide synthase and arginase are major enzymes for the arginine catabolism discovered in heterotrophic organisms. The *C. reinhardtii* genome lacks genes encoding these two enzymes, which might contribute to the N starvation responses of arginine-grown *C. reinhardtii*. To test whether arginine-based growth elicits N starvation responses in photosynthetic organisms with nitric oxide synthase or arginase, we examined a heterokont marine diatom,

Phaeodactylum tricornutum, that has arginase and can grow with arginine as the sole N source (Alonso *et al.,* 2000; Bowler *et al.,* 2008; Allen *et al.,* 2011). As in *C. reinhardtii,* many lipid droplets were found in *P. tricornutum* when grown solely with arginine for five days (Fig. 8). A fluorescence based semi-quantitative assay showed two- to seven-fold higher neutral lipid contents during a seven-day growth period. Similar lipid accumulation suggests that the putative mechanism triggered by arginine cultures may be conserved across diverse photosynthetic organisms.

Discussion

In this report, we showed that arginine cultures display a series of N starvation responses including gametogenesis, induction of N catabolite genes, reduced cellular chlorophyll contents, and an increased carbon flux towards storage without an apparent growth impairment. Thus, arginine cultures may trigger the same signaling that induces N starvation responses during N starvation and help to distinguish N starvation-specific responses from generic stress responses. The N starvation responses in arginine cultures were also observed in a diatom, *P. tricornutum*, suggesting the generalizable effects of the arginine cultures.

How would Chlamydomonas sense N availability?

External N sources are the primary targets for N sensing mechanisms. Plants possess transceptors that combine transporter and sensor functions to sense two primary N sources, NH_4^+ and NO_3^- (Ho *et al.,* 2009; Lanquar *et al.,* 2009; Rogato *et al.,* 2010), but it remains unknown whether their functional homologs exist in *C. reinhardtii*. NH_4^+ sensing antagonizes NO_3^- sensing establishing an NH_4^+ preference in *C. reinhardtii* (Quesada *et al.,* 1993; Quesada & Fernández, 1994). NH_4^+ and NO_3^- ions suppress N starvation responses including gametogenesis without being metabolized (Matsuda *et al.,* 1992; Pozuelo *et al.,* 2000), suggesting that their sensing mechanisms interact with the N starvation

signaling. Nitric oxide generated via nitrate reductase has been suggested to mediate NH_4^+-dependent signaling to suppress NO_3^--dependent signaling (de Montaigu *et al.,* 2010; Chamizo-Ampudia *et al.,* 2017). Nitric oxide is also reported to mediate N starvation-induced cytochrome b_6f degradation (Wei *et al.,* 2014). Whether nitric oxide is also involved in sensing internal N status awaits further study.

In NH_4^+ cultures, the main flux of NH_4^+ is passing through the cytosol to the chloroplast where it is assimilated via the glutamine synthetase (GS)/Fd-glutamate synthase (GOGAT) cycle. *C. reinhardtii* also possesses a cytosolic GS which is predicted to play a minor role in NH_4^+ assimilation as no cytosolic GOGAT is present (Fischer & Klein, 1988). Fluctuating NH_4^+ results in changes in glutamate and α-ketoglutarate levels that are rapidly equilibrated between the cytosol and chloroplast via translocators in the 2-oxoglutarate/malate transporter (OMT) and dicarboxylate transporter (DCT) classes (Weber *et al.,* 1995; Taniguchi *et al.,* 2002; Miura *et al.,* 2004). Accordingly, many amino acids and organic acids, including glutamate and α-ketoglutarate, exhibit drastic reduction during N starvation (Park *et al.,* 2015) and are therefore prime targets for N starvation sensation.

How are N starvation responses triggered in arginine-grown cells?

Arginine is among the many metabolites fluctuating during N starvation and it may directly trigger cellular responses. Bacterial species within *Pseudomonas* and *Streptococcus* possess the arginine catabolism operon, *arcDABC*, whose expression is regulated by the hexameric transcriptional repressor ArgR that forms a complex when bound to arginine (Lim *et al.,* 1987; Gamper *et al.,* 1991; Fulde *et al.,* 2011). In *C. reinhardtii*, the characterized arginine catabolic activities, ADI and citrulline degradation, were shown to be induced in the presence of arginine but also in N-free medium (Sussenbach & Strijkert, 1969).

Arginine catabolic enzymes may be induced by N starvation signals rather than directly by their substrate arginine.

If an arginine-sensing mechanism exists it likely responds to an internal source of arginine rather than an external one as arginine in the environment would be extremely rare. The arginine content transiently rises during the first hour of N starvation together with putrescine and urea, whereas many amino acids and organic acids including glutamate and α-ketoglutarate show drastic reduction (Park *et al.,* 2015). The surge of arginine after N starvation may be caused by a sudden decrease of the chloroplast glutamine pool that releases N-acetyl-L-glutamate kinase (NAGK) from arginine feedback inhibition allowing shuttling of glutamate into arginine biosynthesis (Chellamuthu *et al.,* 2014). This arginine surge would quickly be resolved via activation of arginine catabolism and the restoration of arginine negative inhibition on NAGK. Therefore, if arginine sensing exists it may be involved in triggering the N starvation responses.

Metabolic shifts in arginine-grown cells may hold the key for N starvation sensing

Matsuda *et al.,* (1992) investigated the dedifferentiation of gametes back to vegetative cells by comparing arginine and its precursors, glutamate, glutamine, ornithine, citrulline, and argininosuccinate, together with urea and NH_4^+. This study showed three results: 1) The gametogenesis inducing signal is turned on only in N-free and arginine cultures, 2) The precursors to arginine synthesis from glutamine onward were unable to revert N-starved gametes to vegetative cells despite cell proliferation, and 3) Urea and NH_4^+ immediately revert the gametes into vegetative cells. These results suggest that the catabolism of arginine and arginine precursors will not produce sufficient NH_4^+, at least in the compartment where NH_4^+ is sensed, to suppress gametogenesis. We extend this proposal to N starvation responses in general.

There are three potential ways to produce NH_4^+ during arginine catabolism in *C.*

reinhardtii: the ADI pathway in the chloroplast, the ornithine-putrescine pathway in the peroxisome, and the agmatine pathway in the mitochondria (Fig 7). All three potential NH_4^+ release points occur in organelles and thus the cytosolic NH_4^+ and glutamine concentrations will be lower in arginine-grown cells. This may explain, in part, how arginine growth bypasses the NH_4^+-sensing mechanism that inhibits N starvation responses and gametogenesis. Examination of metabolite profiles between the cytosol and chloroplast in arginine cultures will help to reveal which metabolic pathways are primarily affected and facilitate future investigation of candidate mechanisms for sensing N starvation.

Arginine feeding may drive C_4 photosynthesis in Chlamydomonas

We showed that phototrophic arginine cultures exhibited increased photosynthetic productivity, reduced starch sheath formation, and supported the growth of *cia5* mutants under ambient air condition (Fig. 3B, C & 6). These results suggest that arginine catabolism relieves local CO_2 limitation in the stroma of the chloroplast. However, whether this relief is by direct release of CO_2 or indirect changes in organic acid metabolism remains for further study. Our examination of potential routes of arginine catabolism does not provide a direct source of CO_2 at the vicinity of arginine catabolism (Fig. 7). The lack of arginase and NOS genes and previous biochemical studies suggest that citrulline degradation is the primary route of arginine catabolism and produces unidentified organic acids (Sussenbach & Strijkert 1969, 1970). By co-localization, the previously reported unknown citrulline degradation path may well be the regeneration of arginine from citrulline. Thereby, we propose that ADI and the last two steps of arginine biosynthesis (argininosuccinate synthase and argininosuccinate lyase) form an Arginine-Citrulline cycle (Fig. S6) resembling the Arg-Cit cycle producing nitric oxide in animals (Hecker *et al.,* 1990; Wu & Morris, 1998). Arginine catabolism in *C. reinhardtii* likely relies on the proposed Arg-Cit cycle for which efficient catabolism of citrulline determines how well arginine can be utilized.

What is the primary role of the Arg-Cit cycle in the chloroplast? Our transcriptome survey of the genes encoding the Arg-Cit cycle enzymes suggests that the Arg-Cit cycle will run under N starvation where arginine can be broken down to feed other metabolic pathways such as pyrimidine biosynthesis (Fig. 7; Table S2). The Arg-Cit cycle would also extract amide from aspartate and release fumarate that is readily converted to malate and possibly to oxaloacetate (OAA) via the chloroplastic NADP-malate dehydrogenase (MDH5) (Lemaire *et al.,* 2005). The NADP-MDH in *Arabidopsis* is known to be activated by Fd-TRX when stromal reducing equivalents are used at a reduced rate as in N starvation (Fridlyand *et al.,* 1998). We find it intriguing that malate and OAA could be directly fed into the C_4 carbon fixation pathway via the malic enzyme as in C_4 plants (Kanai & Edwards, 1999). Aspartate synthesis by the chloroplast aspartate aminotransferase (AST3) will consume OAA and glutamate. The reduction in OAA may drive the malate-OAA shuttle bringing OAA into the chloroplast. The catalytic direction of MDH5 towards malate production will occur at very high $NADPH:NADP^+$ levels (Ashton & Hatch, 1983). Any excess malate can be directed through the NADP-malic enzyme (MME5) generating CO_2, reduced $NADP^+$, and a molecule of pyruvate that may enter the gluconeogenesis pathway.

The proposed C_4 carbon fixation may explain how *cia5* can phototrophically grow well in ambient CO_2 conditions and how arginine cultures perform ~50% improved photosynthesis by reducing the photorespiration. In addition, C_4-type carbon fixation predicts twice more ATP consumption than C_3-type carbon fixation, which may explain the increased respiration rate of arginine cultures (Table S3). Direct measurement of photorespiration will help to test out C_4 photosynthesis in the arginine culture.

In the absence of N assimilation from inorganic N sources, photosynthesizing cells may not have enough sink capacity for the high-energy reductants produced

by photosynthetic electron transport. The robust photosynthesis in the arginine cultures is therefore intriguing given this condition. Improved photosynthetic yield of arginine culture may lead to the discovery of a new carbon concentrating mechanism operating under stress conditions resembling the C_4 pathway of plants. Our report about arginine culture provides an essential tool to investigate internal N sensing mechanisms and to test whether specific mechanisms induced by N starvation are critical for tolerating excess photosynthetic reductants resulting from various stress conditions.

Supplementary data

Fig. S1 – Mating efficiency of 21gr and 137c in N-free medium
Fig. S2 – Gametogenesis induced in arginine-grown natural variant strains
Fig. S3 – Expression profile of NIT2-dependent transcriptional marker *THB1*
Fig. S4 – Expression profiles of N starvation marker genes in phototrophic arginine cultures
Fig. S5 – Oxygen evolution in phototrophic arginine cultures
Fig. S6 – Diagram of putative Arginine-Citrulline cycle
Table S1 – Selected N starvation marker genes from available transcriptomes
Table S2 – Metabolic enzymes involved in N flow during arginine catabolism
Table S3 – Oxygen evolution data points for mixo- and phototrophically grown cultures

Acknowledgments
This work was supported by Discovery Grant 418471-12 from the Natural Sciences and Engineering Research Council (NSERC) (to J.-H.L.), by the Korea CCS R&D Center (KCRC), Korean Ministry of Science, grant nos. 2016M1A8A1925345 (to J.-H.L.), 2014M1A8A1049278 (to S.J.S.) and 2014M1A8A1049273 (to E.J.).

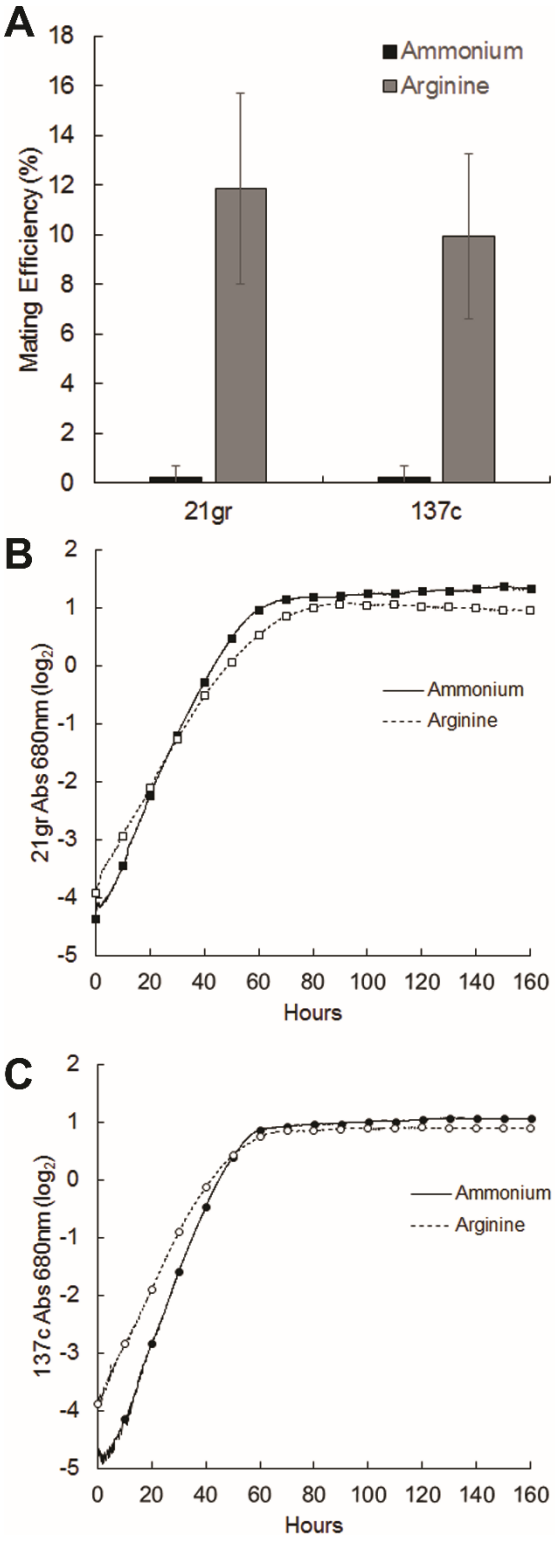

Fig. 1 - Gametogenesis is induced during growth in arginine cultures. (A) Mating efficiencies in cells grown 10 days on L-Arg or NH_4^+ TAP agar plates and resuspended in 1 mL of liquid L-Arg or NH_4^+ TAP for 24 hrs. Data represents the mean ± the standard deviation from three biological replicates. (B & C) Bioreactor

optical density (680 nm) growth curves on a $\log_2$ scale of 80 mL cultures bubbled with ambient air for strain 21gr and 137c, respectively. Dashed lines represent cultures grown with 8 mM L-Arg as the sole N source and solid lines represent cultures grown with 8 mM NH_4^+ as the sole N source.

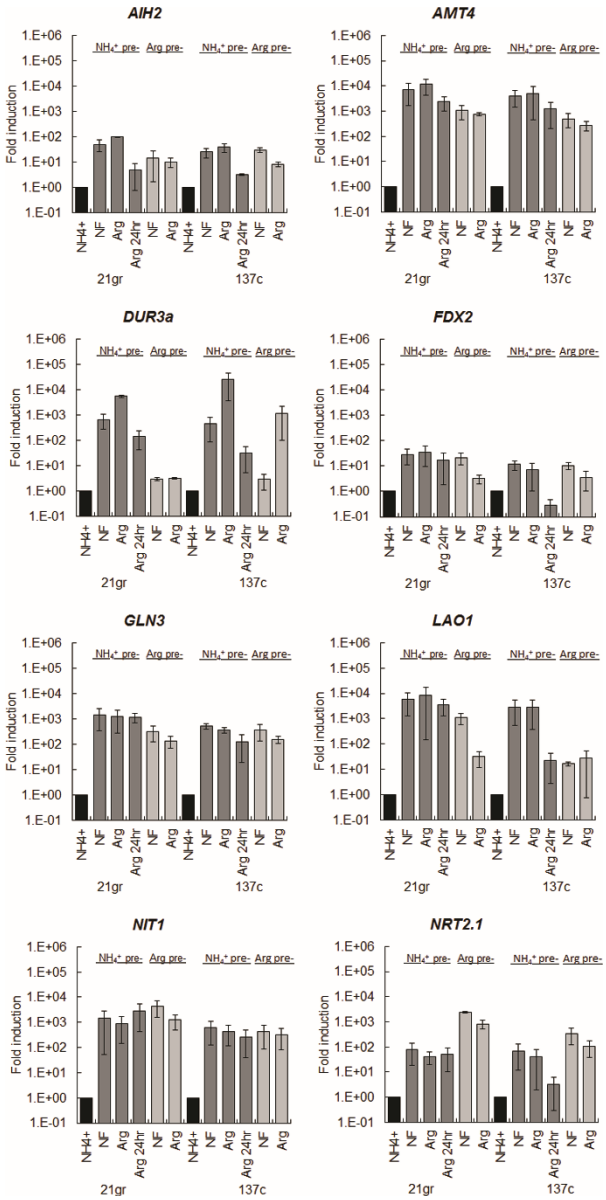

Fig. 2 - Arginine cultured cells comparably upregulate N starvation marker genes. NH_4^+ (dark gray) or L-Arg (light gray) TAP grown cultures of 21gr and 137c strains were harvested at mid-log phase, washed with N-free TAP, and incubated in NH_4^+, L-Arg, or N-free TAP for two or twenty-four hours. Expression profiling with RT-qPCR was performed using RNA extracted following the incubation. Data represent the mean ± the standard deviation from three biological replicates.

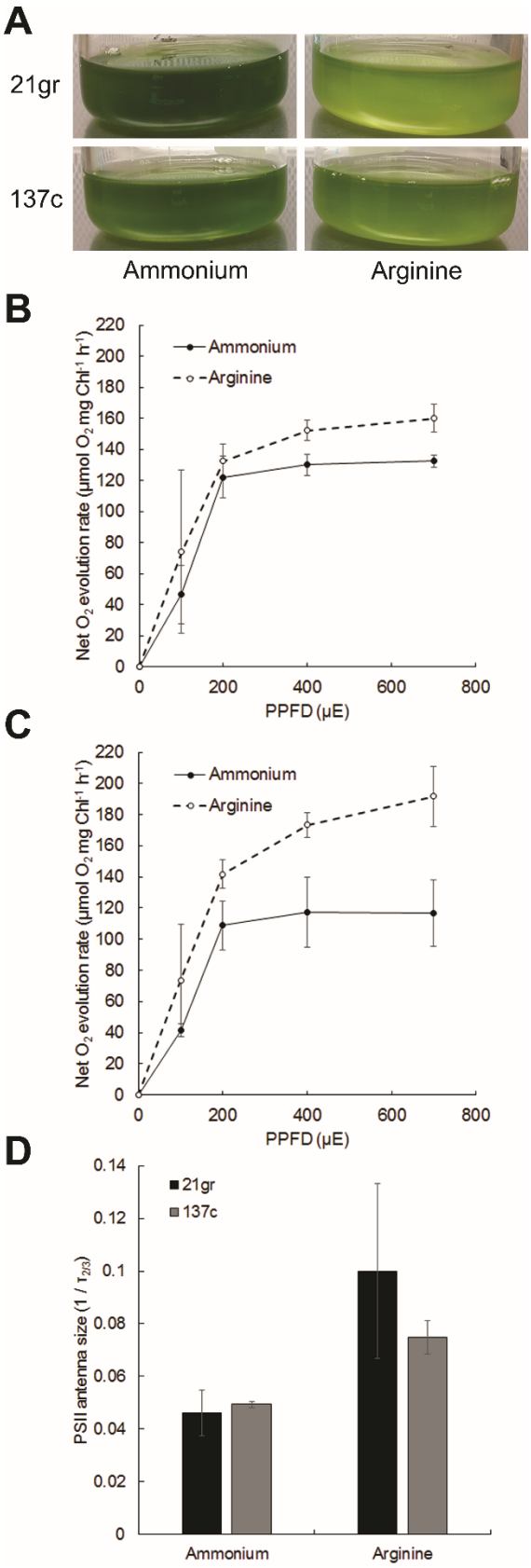
A
21gr
137c
Ammonium
Arginine
B
Ammonium
Arginine
Net O2 evolution rate (µmol O2 mg Chl-1 h-1)
PPFD (µE)
C
Ammonium
Arginine
Net O2 evolution rate (µmol O2 mg Chl-1 h-1)
PPFD (µE)
D
21gr
137c
PSII antenna size (1 / τ2/3)
Ammonium
Arginine

764

Fig. 3 - Oxygen evolution is more efficient in arginine cultures despite reduced chlorophyll and increased antenna size. (A) Early log phase cultures (2×10^6 cells per mL) demonstrate a pale green color indicative of reduced chlorophyll when L-Arg is used as the sole N source rather than NH_4^+. (B) & (C) Oxygen evolution per mg of chlorophyll is significantly higher at saturating light intensity when L-Arg is used as the sole N source for both the 21gr and 137c strains, respectively. (D) PSII antenna size is greater for both 21gr and 137c in L-Arg cultures compared to NH_4^+ cultures. The inverse of the time required to reach 2/3 of the maximum fluorescence ($\tau_{2/3}$) following addition of DCMU is proportional to PSII antenna size. Data for (B), (C), and (D) represent the mean ± the standard deviation from two biological replicates.

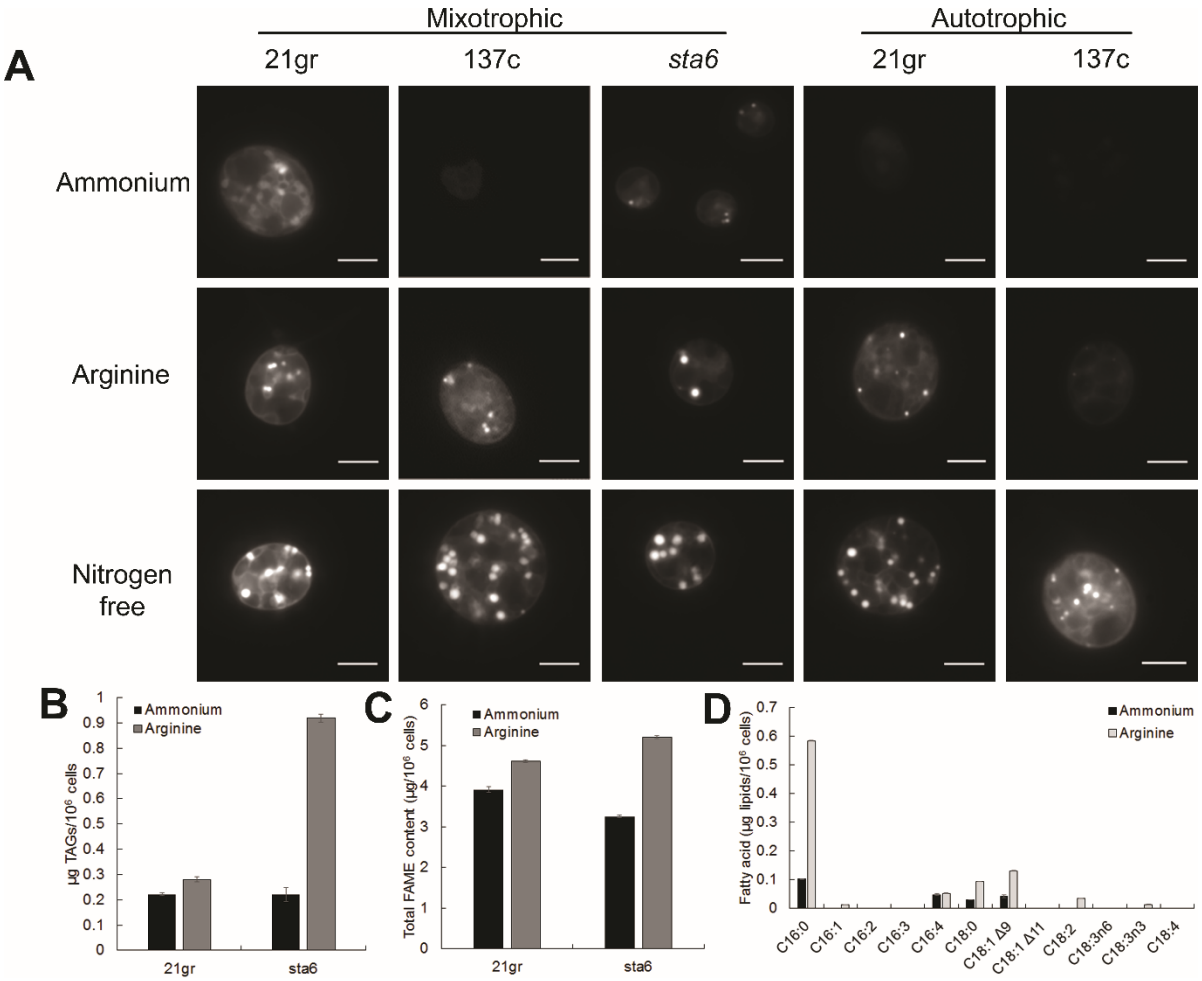

Fig. 4 - Neutral lipid biosynthesis is induced in cells grown with arginine. (A) Micrographs of Nile red stained mid-log phase cells from NH_4^+ or L-Arg cultures grown either mixotrophically or phototrophically alongside cells starved of N for 3 days captured using a 100x objective. The starchless mutant, *sta6,* was used as a high lipid accumulating control line. Scale bar represents 5 µm. (B & C) TAG and FAME quantification using gas chromatography of wild type 21gr and *sta6* grown mixotrophically to mid-log phase using either NH_4^+ or L-Arg. (D) Lipid profiling of TAGs from mid-log phase *sta6* cultures grown mixotrophically in either NH_4^+ or L-Arg.

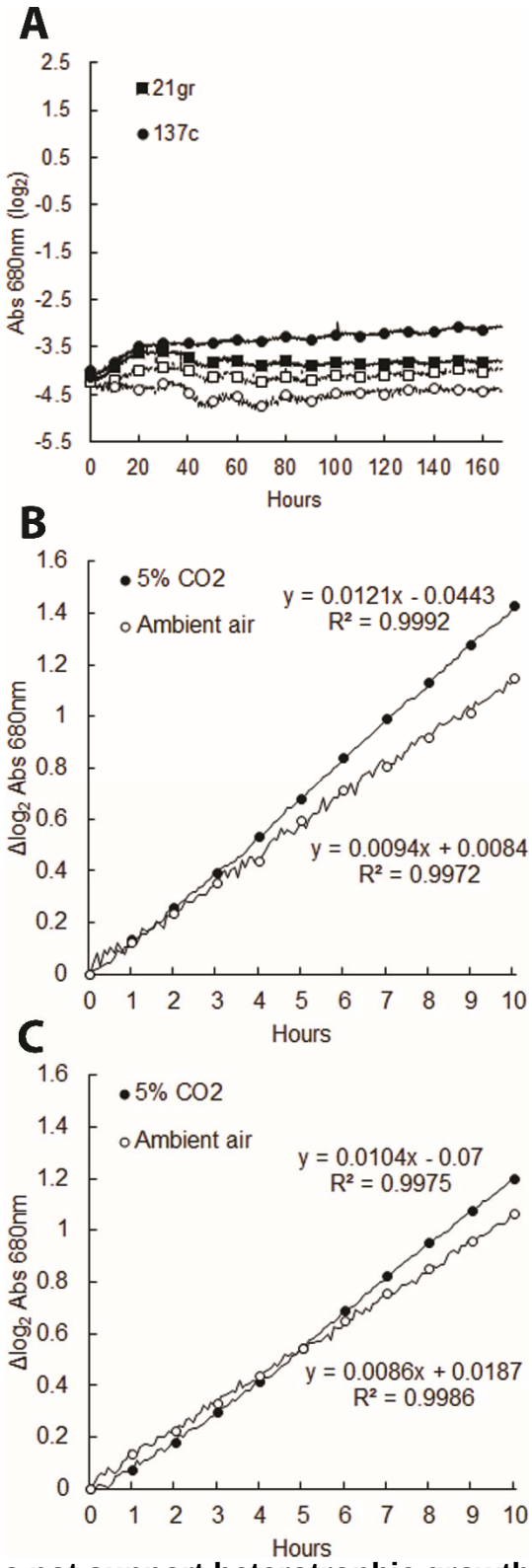

Fig. 5 - Arginine does not support heterotrophic growth nor does additional CO_2 improved phototrophic growth. (A) Strains 21gr (squares) and 137c (circles) incubated with 8 mM L-Arg (open symbols) or NH_4^+-TAP (closed symbols) and bubbled with 5% CO_2 and dim light (<10 µmol m^{-2} s^{-1}). Strain 21gr

(B) and 137c (C) grown with 8 mM L-Arg and bubbled with 5% CO_2 (closed symbols) or ambient air (open symbols) and high light (250 µmol m^{-2} s^{-1}). Bioreactor growth rates determined by the change in optical density at 680 nm on a log_2 scale over 10 hours of linear growth during the mid-log phase of 80 mL cultures.

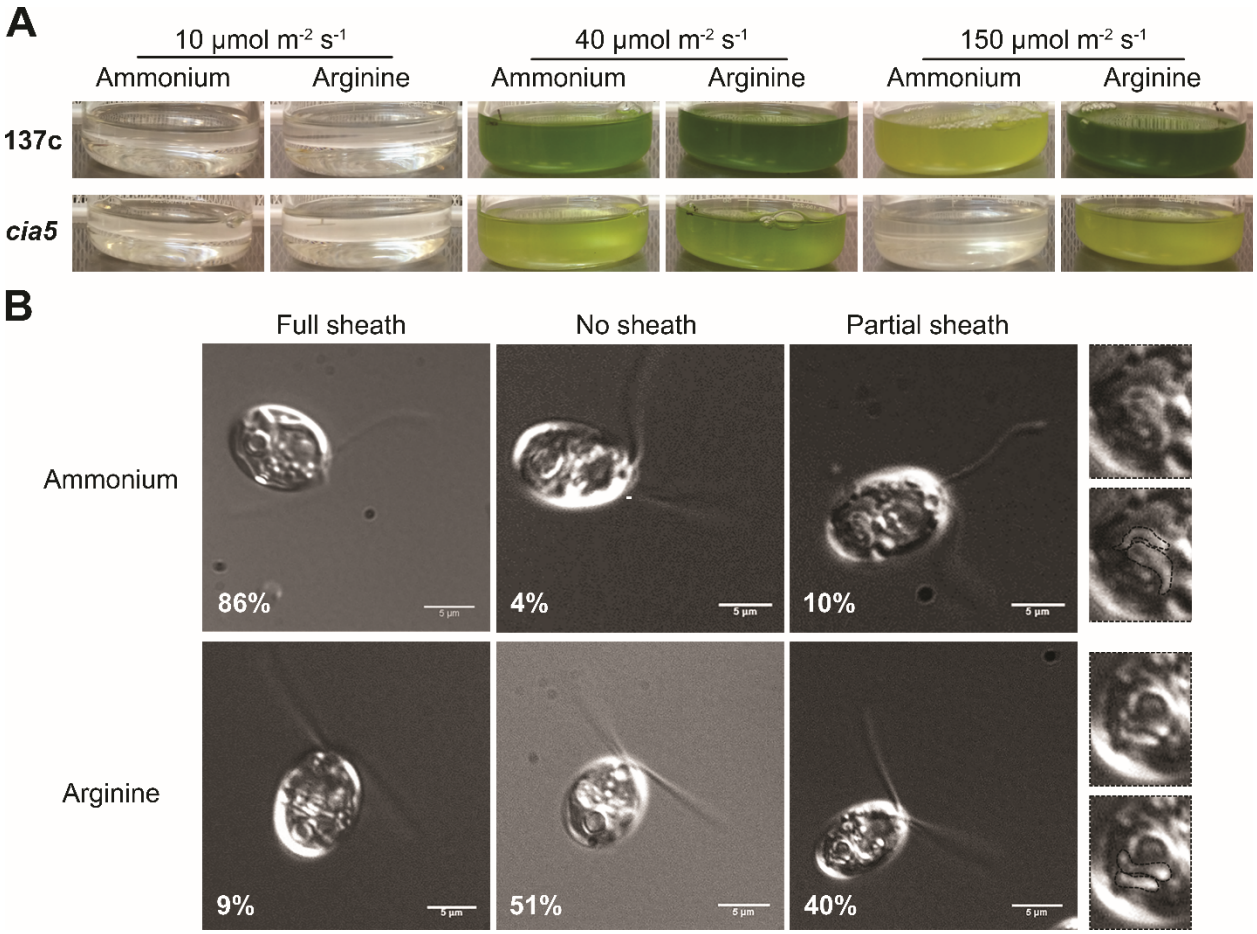

Fig. 6 - Carbon concentration mechanism is not required for high light growth in arginine. (A) A mutant defective in activation of the CCM (*cia5*) can grow under high light using L-Arg but not NH_4^+. Photographs of cultures were taken after seven days of growth in phototrophic medium. (B) Micrographs of representative cells indicating CCM formation of a starch sheath around the pyrenoid from mid-log phase cultures grown with high light (150 µmol m^{-2} s^{-1}) in either NH_4^+ or L-Arg using a 100x objective. Scale bar represents 5 µm and the percent indicates how many cells out of 100 show the represented phenotype for NH_4^+ or L-Arg cultures. The images to the right are enlarged from the partial sheath images to draw attention to the abnormal sheath formation (outlined by the dashed line).

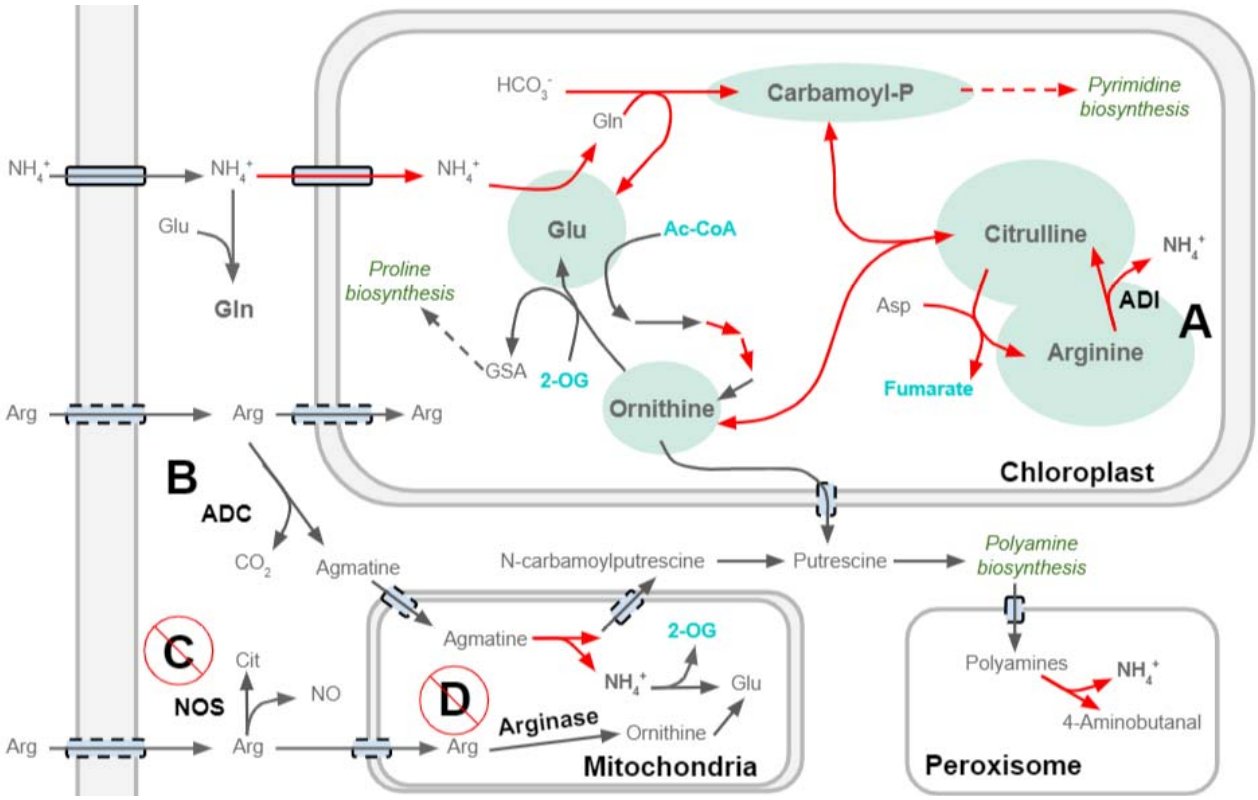

Fig. 7 – *In silico* reconstruction of N flow during arginine catabolism in *C. reinhardtii*. Two enzymes, A) Arginine deiminase (Cre08.g360350) and B) Arginine decarboxylase (putative genes; Cre02.g105150, Cre16.g675900) are potential gates of arginine catabolism as no genes/proteins have been found for C) Nitric oxide synthase or D) Arginase. Solid arrows represent individual enzymatic steps with red arrows representing corresponding genes upregulated following N starvation. Dashed arrows represent pathways with multiple enzymatic steps. Green text delineates potential metabolic destinations (or sinks) accepting N from arginine catabolism. Dashed lines around proteins indicate transporters that have not been identified/functionally characterized in *C. reinhardtii.* Detailed gene and expression information is provided in Table S2.

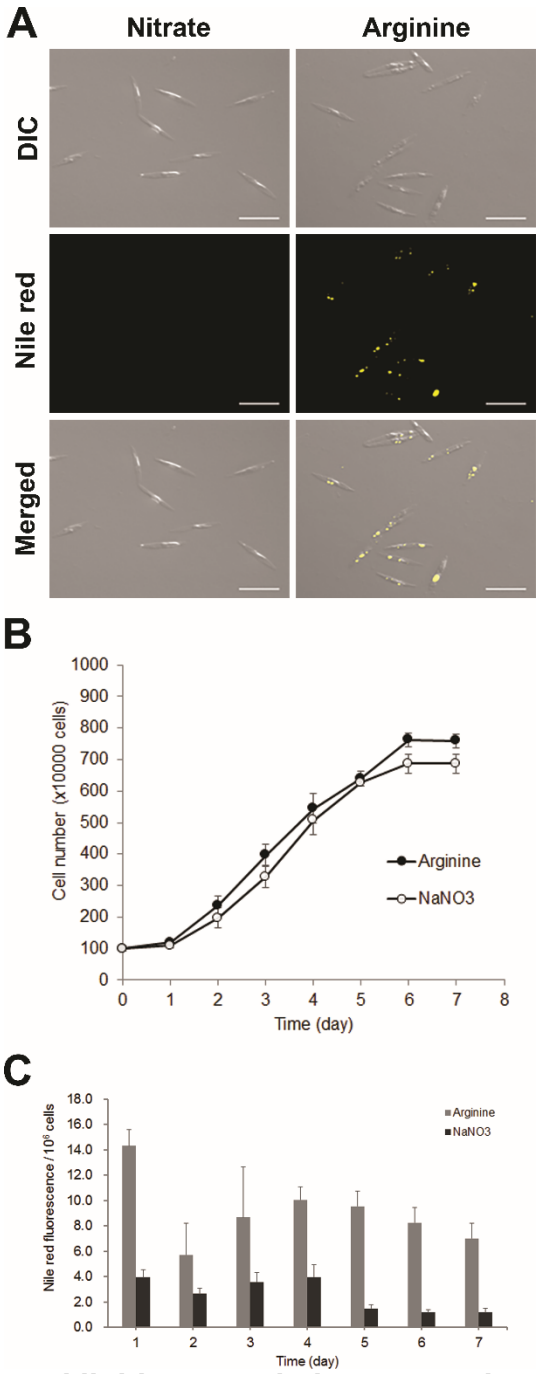

Fig. 8 - Increased neutral lipid accumulation occurs in arginine grown diatom, *Phaeodactylum tricornutum*. (A) Micrographs of Nile red stained cells from cultures grown for seven days with the standard $NaNO_3$ or L-Arg as the sole N source grown. Bar = 20 µm. (B) Culture proliferation measured by cell counting with a hemocytometer for cultures grown with L-Arg (closed circles) or NO_3^- as the sole N source (open circles). Average from triplicate sampling in two independent experiments. (C) Semi-quantitative determination of total neutral lipid accumulation per 10^6 cells using a fluorescence-based assay comparing

overall Nile red fluorescence between $NaNO_3$ or L-Arg cultures. Average from triplicate sampling in two independent experiments.

Table 1. Properties of C. reinhardtii cells acclimated to different nitrogen sources in mixotrophic condition. Cells from mid-log mixotrophic cultures used to determine the F_V / F_M, $\Phi_{PSII,}$ Chl a/b ratio, and total Chl (nmol/10^6 cells). (n = 2; values shown are means ± standard deviation)

Strain	F_V / F_M		Φ_{PSII}		Chl a/b		Total Chl (nmol/10^6 cells)	
	Ammonium	Arginine	Ammonium	Arginine	Ammonium	Arginine	Ammonium	Arginine
21gr	0.75 ± 0.02	0.76 ± 0.01	0.51 ± 0.10	0.57 ± 0.06	2.35 ± 0.18	2.78 ± 0.22	3.47 ± 0.50	1.18 ± 0.46
137c	0.74 ± 0.02	0.73 ± 0.01	0.57 ± 0.01	0.55 ± 0.04	2.65 ± 0.06	2.83 ± 0.05	2.64 ± 0.40	1.78 ± 0.06

Table 2. Properties of C. reinhardtii cells acclimated to different nitrogen sources in phototrophic condition. Cells from mid-log phototrophic cultures used to determine the F_V / F_M, Φ_{PSII}, Chl a/b ratio, and total Chl (nmol/10^6 cells). (n = 2; values shown are means ± standard deviation)

Strain	F_V / F_M		Φ_{PSII}		Chl a/b		total Chl (nmol/10^6 cells)	
	Ammonium	Arginine	Ammonium	Arginine	Ammonium	Arginine	Ammonium	Arginine
21gr	0.50 ± 0.06	0.58 ± 0.01	0.32 ± 0.05	0.39 ± 0.01	2.61 ± 0.12	2.71 ± 0.10	2.28 ± 0.07	2.56 ± 0.37
137c	0.56 ± 0.05	0.64 ± 0.03	0.37 ± 0.06	0.45 ± 0.04	2.94 ± 0.13	2.81 ± 0.07	2.50 ± 0.33	2.11 ± 0.57

References

Allen MD, Kropat J, Tottey S, Del Campo JA, Merchant SS. 2007. Manganese deficiency in *Chlamydomonas* results in loss of photosystem II and MnSOD function, sensitivity to peroxides, and secondary phosphorus and iron deficiency. Plant Physiology **143,** 263-277.

Allen A, Dupont C, Oborník M, Horák A, Nunes-Nesi A, Mccrow J, Zheng H, Johnson D, Hu H, Fernie A, Bowler C. 2011. Evolution and metabolic significance of the urea cycle in photosynthetic diatoms. Nature **473,** 203-207.

Alonso DL, Belarbi EH, Fernández-Sevilla JM, Rodríguez-Ruiz J, Grima EM. 2000. Acyl lipid composition variation related to culture age and nitrogen concentration in continuous culture of the microalga *Phaeodactylum tricornutum*. Phytochemistry **54,** 461-471.

Amory AM, Vanlerberghe GC, Turpin DH. 1991. Demonstration of both a photosynthetic and a nonphotosynthetic CO_2 requirement for NH_4^+ assimilation in the green algae *Selenastrum minutum*. Plant Physiology **95,** 192-196.

Arnon D. 1949. Copper enzymes in isolated chloroplasts. Polyphenoloxidase in *Beta vulgaris*. Plant Physiology **24,** 1-15.

Ashton AR, Hatch MD. 1983. Regulation of C_4 photosynthesis: Regulation of activation and inactivation of NADP-malate dehydrogenase by NADP and NADPH. Archives of Biochemistry and Biophysics **227,** 416-424.

Baker NR. 2009. Chlorophyll fluorescence: a probe of photosynthesis *in vivo*. Annual Review of Plant Biology **59,** 89-113.

Bell E, Malmberg R. 1990. Analysis of a cDNA encoding arginine decarboxylase from oat reveals similarity to the *Escherichia coli* arginine decarboxylase and evidence of protein processing. Molecular & General Genetics **244,** 431-436.

Bligh EG, Dyer WJ. 1959. A rapid method of total lipid extraction and purification. Canadian Journal of Biochemistry and Physiology **37,** 911-917.

Bowler C, Allen A, Badger J *et al.* 2008. The *Phaeodactylum* genome reveals the evolutionary history of diatom genomes. Nature **456,** 239-244.

Bulté L, Wollman FA. 1992. Evidence for a selective destabilization of an integral membrane protein, the cytochrome *b_6/f* complex, during gametogenesis in *Chlamydomonas reinhardtii*. European Journal of Biochemistry **204,** 327-336.

Cain J. 1965. Nitrogen utilization in 38 freshwater Chlamydomonad algae. Canadian Journal of Botany **43,** 1367-1378.

Chalker-Scott, L. 1999. Environmental significance of anthocyanins in plant stress response. Photochemistry and Photobiology **70,** 1-9.

Chamizo-Ampudia A, Sanz-Luque E, Llamas A, Galván A, Fernández E. 2017. Nitrate reductase regulates plant nitric oxide homeostasis. Trends in Plant Science **22,** 163-174.

Chellamuthu VR, Ermilova E, Lapina T, Lüddecke J, Minaeva E, Herrmann C, Hartmann MD, Forchhammer K. 2014. A widespread glutamine-sensing mechanism in the plant kingdom. Cell **20,** 1188-1199.

Cohen E, Arad S, Heimer Y, Mizrahi Y. 1983. Polyamine biosynthetic enzymes in *Chlorella*: characterization of ornithine and arginine decarboxylase. Plant and Cell Physiology **24,** 1003-1010.

Cooper TG. 1982. Nitrogen metabolism in *Saccharomyces cerevisiae*. In: Strathern JN, Jones EW, Broach J, eds. *The molecular biology of the yeast Saccharomyces: metabolism and gene expression*. Cold Spring Harbor NY, Cold Spring Harbor Laboratory, 39-99.

de Bianchi S, Dall'Osto L, Tognon G, Morosinotto T, Bassi R. 2008. Minor antenna proteins CP24 and CP26 affect the interactions between photosystem II subunits and the electron transport rate in grana membranes of *Arabidopsis*. The Plant Cell **20,** 1012-1028.

de Montaigu A, Sanz-Luque E, Galván A, Fernández E. 2010. A soluble guanylate cyclase mediates negative signaling by ammonium on expression of nitrate reductase in *Chlamydomonas.* The Plant Cell **22,** 1532-1548.

Diaz C, Saliba-Colombani V, Loudet O, Belluomo P, Moreau L, Daniel-Vedele F, Morot-Gaudry JF, Masclaux-Daubresse C. 2006. Leaf yellowing and anthocyanin accumulation are two genetically independent strategies in response to nitrogen limitation in *Arabidopsis thaliana*. Plant and Cell Physiology **47,** 74-83.

Ding L, Wang KJ, Jiang GM, Biswas DK, Xu H, Li LF, Li YH. 2005. Effects of nitrogen deficiency of photosynthetic traits of maize hybrids released in different years. Annals of Botany **96,** 925-930.

Fischer P, Klein U. 1988. Localization of nitrogen-assimilating enzymes in the chloroplast of *Chlamydomonas reinhardtii*. Plant Physiology **88,** 947-952.

Fridlyand LE, Backhausen JE, Scheibe R. 1998. Flux control of the malate valve in leaf cells. Archives of Biochemistry and Biophysics **349,** 290-298.

Fulde M, Willenborg J, de Greeff A, Benga L, Smith H, Valentin-Weigand P, Goethe R. 2011. ArgR is an essential local transcriptional regulator of the arcABC operon in *Streptococcus suis* and is crucial for biological fitness in an acidic environment. Microbiology **157,** 572-582.

Galloway RE, Goodenough UW. 1985. Genetic analysis of mating locus linked mutations in *Chlamydomonas reinhardtii*. Genetics **111,** 447-461.

Gamper M, Zimmermann A, Haas D. 1991. Anaerobic regulation of transcription initiation in the arcDABC operon of *Pseudomonas aeruginosa*. Journal of Bacteriology **173,** 4742-4750.

Gorman D, Levine R. 1965. Cytochrome f and plastocyanin: their sequence in the photosynthetic electron transport chain of *Chlamydomonas reinhardi.* Proceedings of the National Academy of Sciences of the United States of America **54,** 1665-1669.

Hanfrey C, Sommer S, Mayer M, Burtin D, Michael A. 2001. *Arabidopsis* polyamine biosynthesis: absence of ornithine decarboxylase and the mechanism of arginine decarboxylase activity. The Plant Journal **27,** 551-560.

Hecker M, Sessa W, Harris H, Anggård E, Vane J. 1990. The metabolism of L-arginine and its significance for the biosynthesis of endothelium-derived relaxing factor: cultured endothelial cells recycle L-citrulline to L-arginine. Proceedings of the National Academy of Sciences of the United States of America **87,** 8612-8616.

Ho C, Lin S, Hu H, Tsay Y. 2009. CHL1 functions as a nitrate sensor in plants. Cell **138,** 1184-1194.

Honeycutt RC, Margulies MM. 1972. Control of ribosome content, gamete formation and amino acid uptake in wild-type and arg-1 *Chlamydomonas reinhardti*i. Biochimica et Biophysica Acta **281,** 399-405.

Hu Q, Sommerfeld M, Jarvis E, Ghirardi M, Posewitz M, Seibert M, Darzins A. 2008. Microalgal triacylglycerols as feedstocks for biofuel production: perspectives and advances. The Plant Journal **54,** 621-639.

Huppe HC, Turpin DH. 1994. Integration of carbon and nitrogen metabolism in plant and algal cells. Annual Review of Plant Biology **45,** 577-607.

Huergo LF, Chandra G, Merrick M. 2013. PII signal transduction proteins: nitrogen regulation and beyond. FEMS Microbiology Review **37,** 251-283.

Johnson X, Vandystadt G, Bujaldon S, Wollman F, Dubois R, Roussel P, Alric J, Béal D. 2009. A new setup for in vivo fluorescence imaging of photosynthetic activity. Photosynthesis Research **102,** 85-93.

Johnson X, Alric J. 2013. Central carbon metabolism and electron transport in *Chlamydomonas reinhardtii*: metabolic constraints for carbon partitioning between oil and starch. Eukaryotic Cell **12,** 776-793.

Johnson E, Rice S, Preimesberger M, Nye D, Gilevicius L, Wenke B, Brown J, Witman G, Lecomte J. 2014. Characterization of THB1 a *Chlamydomonas reinhardtii* truncated hemoglobin: linkage to nitrogen metabolism and identification of lysine as the distal heme ligand. Biochemistry **53,** 4573-4589.

Joo S, Nishimura Y, Cronmiller E, Hong RH, Kariyawasam T, Wang MH, Shao NC, Akkad SE, Suzuki T, Higashiyama T, Jin E, Lee JH. 2017. Gene regulatory networks for the haploid-to-diploid transition of *Chlamydomonas reinhardtii.* Plant Physiology **175**, 314-332.

Kanai R, Edwards G. 1999. The biochemistry of C_4 photosynthesis. In: Sage RF, Monson RK, eds. *C_4 plant biology*. San Diego, CA: Academic Press, 49-87.

Kim JYH, Kwak HS, Sung YJ, Choi HI, Hong ME, Lim HS, Lee JH, Lee SY, Sim SJ. 2016. Microfluidic high-throughput selection of microalgal strains with superior photosynthetic productivity using competitive phototaxis. Scientific Reports doi: 10.1038/srep21155.

Kirk DL, Kirk MM. 1978. Carrier-mediated uptake of arginine and urea by *Chlamydomonas reinhardtii*. Plant Physiology **61,** 556-560.

Kirst H, Garcia-Cerdan J, Zurbriggen A, Melis A. 2012. Assembly of the light-harvesting chlorophyll antenna in the green alga *Chlamydomonas reinhardtii* requires expression of the TLA2 CpFTSY gene. Plant Physiology **158,** 930-945.

Lanquar V, Loqué D, Hörmann F, Yuan L, Bohner A, Engelsberger WR, Lalonde S, Schulze WX, von Wirén N, Frommer WB. 2009. Feedback inhibition of ammonium uptake by a phosphor-dependent allosteric mechanism in *Arabidopis.* The Plant Cell **21,** 3610-3622.

Lee DY, Park JJ, Barupal DK, Fiehn O. 2012. System response of metabolic networks in *Chlamydomonas reinhardtii* to total available ammonium. Molecular & Cellular Proteomics **11,** 973-988.

Lemaire SD, Quesada A, Merchan F, Corral JM, Igeno MI, Keryer E, Issakidis-Bourguet E, Hirasawa M, Knaff DB, Miginiac-Maslow M. 2005. NADP-malate dehydrogenase from unicellular green alga *Chlamydomonas reinhardtii.* A first step toward redox regulation? Plant Physiology **137,** 514-521.

Li X, Moellering ER, Liu B, Johnny C, Fedewa M, Sears BB, Kuo MH, Benning C. 2012. A galactoglycerolipid lipase is required for triacylglycerol accumulation and survival following nitrogen deprivation in *Chlamydomonas reinhardtii*. Plant Cell **24,** 4670-4686.

Lim D, Oppenheim J, Eckhardtt T, Maas W. 1987. Nucleotide sequence of the argR gene of *Escherichia coli* K-12 and isolation of its product, the arginine repressor. Proceedings of the National Academy of Sciences **84,** 6697-6701.

Lim HY, Kim JYH, Kwak HS, Sim SJ. 2014. Integrated Microfluidic Platform for Multiple Processes from Microalgal Culture to Lipid Extraction. Analytical Chemistry **86,** 8585-8592.

Loppes R. 1969. A new class of arginine-requiring mutants in *Chlamydomonas reinhardi*. Molecular and General Genetics **104,** 172-177.

Mackinder LCM, Chen C, Leib RD, Patena W, Blum SR, Rodman M, Ramundo S, Adams CM, Jonikas MC. 2017. A spatial interactome reveals the

protein organization of the algal CO_2-concentrating mechanism. Cell **171,** 133-147.

Martin N, Goodenough U. 1975. Gametic differentiation in *Chlamydomonas reinhardtii.* I. Production of gametes and their fine structure. The Journal of Cell Biology **67,** 587-605.

Matsuda Y, Shimada T, Sakamoto Y. 1992. Ammonium ions control gametic differentiation and dedifferentiation in *Chlamydomonas reinhardtii*. Plant and Cell Physiology **33,** 909-914.

Melis A, Spangfort M, Andersson B. 1987. Light-absorption and electron-transport balance between photosystem II and photosystem I in spinach chloroplasts. Photochemistry and Photobiology **45,** 129-136.

Miller R, Wu G, Desphande RR, *et al.* 2007. Proposed carbon dioxide concentrating mechanism in *Chlamydomonas reinhardtii*. Eukaryotic Cell **6,** 1251-1269.

Miura K, Yamano T, Yoshioka S, *et al.* 2004. Expression profiling-based identification of CO_2-responsive genes regulated by CCM1 controlling a carbon-concentrating mechanism in *Chlamydomonas reinhardtii.* Plant Physiology **135,** 1595-1607.

Moroney J, Ynalvez R. 2007. Proposed carbon dioxide concentrating mechanism in *Chlamydomonas reinhardtii*. Eukaryotic Cell **6,** 1251-1259.

Muñoz-Blanco J, Hidalgo-Martinez J, Cárdenas J. 1990. Extracellular deamination of L-amino acids by *Chlamydomonas reinhardtii* cells. Planta **182,** 194-198.

Oginsky E, Gehrig R. 1952. The arginine dihydrolase system of *Streptococcus faecalis*. II. Properties of arginine desimidase. The Journal of Biological Chemistry **198,** 799-805.

Ono K, Terashima I, Watanabe A. 1996. Interaction between nitrogen deficit of a plant and nitrogen content in the old leaves. Plant and Cell Physiology **37,** 1083-1089.

Park JJ, Wang H, Gargouri M, Deshpande RR, Skepper JN, Holguin O, Juergens MT, Shachar-Hill Y, Hicks LM. 2015. The response of

Chlamydomonas reinhardtii to nitrogen deprivation: a systems biology analysis. The Plant Journal **81,** 611-624.

Petrack B, Sullivan L, Ratner S. 1957. Behavior of purified arginine desiminase from *S. faecalis*. Archives of Biochemistry and Biophysics **69,** 186-197.

Piedras P, Pineda M, Muñoz J, Cárdenas J. 1992. Purification and characterization of an L-amino-acid oxidase from *Chlamydomonas reinhardtii*. Planta **188,** 13-18.

Pozuelo M, Merchán F, Macías MI, Beck CF, Galván A, Fernández E. 2000. The negative effect of nitrate on gametogenesis is independent of nitrate assimilation in *Chlamydomonas reinhardtii*. Planta **211,** 287-292.

Quesada A, Galván A, Schnell RA, Lefebvre PA, Fernández E. Five nitrate assimilation-related loci are clustered in *Chlamydomonas reinhardtii*. Molecular and General Genetics **240,** 387-394.

Quesada A, Fernández E. 1994. Expression of nitrate assimilation related genes in *Chlamydomonas reinhardtii*. Plant Molecular Biology **24,** 185-194.

Ramazanov Z, Rawat M, Henk MC, Mason CB, Matthews SW, Moroney JV. 1994. The induction of the CO_2-concentrating mechanism is correlated with the formation of the starch around the pyrenoid of *Chlamydomonas reinhardtii*. Planta **195,** 210-216.

Rodolfi L, Zittelli GC, Bassi N, Padovani G, Biondi N, Bonini G, Tredici MR. 2009. Microalgae for oil: strain selection, induction of lipid synthesis and outdoor mass cultivation in a low-cost photobioreactor. Biotechnology and Bioengineering **102,** 100-112.

Rogato A, D'Apuzzo E, Chiurazzi M. 2010. The multiple plant response to high ammonium conditions: The *Lotus japonicus* AMT1; 3 protein acts a putative transceptor. Plant signaling & behavior **5,** 1594-1596.

Sager R, Granick S. 1953. Nutritional studies with *Chlamydomonas reinhardi*. Annals of the New York Academy of Sciences **56,** 831-838.

Sager R, Granick S. 1954. Nutritional control of sexuality in *Chlamydomonas reinhardi*. The Journal of General Physiology **37,** 729-742.

Schmollinger S, Mühlhaus T, Boyle NR, *et al.* 2014. Nitrogen-sparing mechanisms in *Chlamydomonas* affect the transcriptome, the proteome, and photosynthetic metabolism. Plant Cell **26,** 1410-1435.

Siersma P, Chiang K. 1971. Conservation and degradation of cytoplasmic and chloroplast ribosomes in *Chlamydomonas reinhardtii*. Journal of Molecular Biology **58,** 167-185.

Sussenbach J, Strijkert P. 1969. Arginine metabolism in *Chlamydomonas reinhardi* arginine deiminase: The first enzyme of the catabolic pathway. FEBS Letters **3,** 166-168.

Sussenbach J, Strijkert P. 1970. Arginine metabolism in *Chlamydomonas reinhardi.* A new type of citrulline degradation. FEBS Letters **7,** 274-276.

Syrett PJ. 1953a. The assimilation of ammonia by nitrogen-starved cells of *Chlorella vulgaris*: Part I. Annals of Botany **17,** 1-20.

Syrett PJ. 1953b. The assimilation of ammonia by nitrogen-starved cells of *Chlorella vulgaris*: Part II. Annals of Botany **17,** 21-36.

Taniguchi M, Taniguchi Y, Kawasaki M, Takeda S, Kato T, Sato S, Tabata S, Miyake H, Sugiyama T. 2002. Identifying and characterizing plastidic 2-oxoglutarate/malate and dicarboxylate transporters in *Arabidopsis thaliana*. Plant and Cell Physiology **43,** 706-717.

Tardif M, Atteia A, Specht M, *et al.* 2012. PredAlgo: a new subcellular localization prediction tool dedicated to green algae. Molecular Biology and Evolution **29,** 3625-3639.

Terashima M, Specht M, Naumann B, Hippler M. 2010. Characterizing the anaerobic response of *Chlamydomonas reinhardtii* by quantitative proteomics. Molecular and Cellular Proteomics **9,** 1514-1532.

Tsai CH, Warakanont J, Takeuchi T, Sears BB, Moellering ER, Benning C. 2014. The protein Compromised Hydrolysis of Triacylglycerols 7 (CHT7) acts as a repressor of cellular quiescence in *Chlamydomonas*. Proceedings of the National Academy of Sciences of the United States of America **111,** 15833-15838.

Turpin DH, Elrifi IR, Birch DG, Weger HG, Holmes JJ. 1988. Interactions between photosynthesis, respiration, and nitrogen assimilation in microalgae. Canadian Journal of Botany **66,** 2083-2097.

Vallon O, Bulté L, Kuras R, Olive J, Wollman FA. 1993. Extensive accumulation of an extracellular L-amino-acid oxidase during gametogenesis of *Chlamydomonas reinhardtii*. European Journal of Biochemistry **215,** 351-360.

Van K, Wang Y, Nakamura Y, Spalding MH. 2001. Insertional mutants of *Chlamydomonas reinhardtii* that require elevated CO_2 for survival. Plant Physiology **127,** 607-614.

Wang Y, Sun Z, Horken KM, Im CS, Xiang Y, Grossman AR, Weeks DP. 2005. Analyses of CIA5, the master regulator of the carbon-concentrating mechanism in *Chlamydomonas reinhardtii*, and its control of gene expression. Canadian Journal of Botany **83,** 765-779.

Wase N, Black PN, Stanley BA, DiRusso CC. 2014. Integrated quantitative analysis of nitrogen stress response in *Chlamydomonas reinhardtii* using metabolite and protein profiling. Journal of Proteome Research **13,** 1373-1396.

Weber A, Menzlaff E, Arbinger B, Gutensohn M, Eckerskorn C, Fluegge UI. 1995. The 2-oxoglutarate/malate translocator of chloroplast envelope membranes: molecular cloning of a transporter containing a 12-helix motif and expression of the functional protein in yeast cells. Biochemistry **34,** 2621-2627.

Weers P, Gulati R. 1997. Growth and reproduction of *Daphnia galeata* in response to changes in fatty acids, phosphorus, and nitrogen in *Chlamydomonas reinhardtii*. Limnology and Oceanography **42,** 1584-1589.

Wei L, Derrien B, Gautier A, *et al.* 2014. Nitric oxide-triggered remodeling of chloroplast bioenergetics and thylakoid proteins upon nitrogen starvation in *Chlamydomonas reinhardtii*. The Plant Cell **26,** 353-372.

Winter G, Todd CD, Trovato M, Forlani G, Funck D. 2015. Physiological implications of arginine metabolism in plants. Front Plant Sci **6,** 534.

Wu G, Morris SM. 1998. Arginine metabolism: nitric oxide and beyond. Biochemical Journal **336,** 1-17.

Xue J, Niu YF, Huang T, Yang WD, Liu JS, Li HY. 2015. Genetic improvement of the microalga *Phaeodactylum tricornutum* for boosting neutral lipid accumulation. Metabolic engineering **27,** 1-9.

Zhang W, Du G, Zhou J, Chen J. 2018. Regulation of sensing, transportation, and catabolism of nitrogen sources in *Saccharomyces cerevisiae*. Microbiology and Molecular Biology Reviews doi: 10.1128/MMBR.00040-17.